

DC-Bias-free Surface Potential Measurements by Heterodyne AC Kelvin Probe Force Microscopy

Thomas Hackl, Mathias Poik and Georg Schitter *Senior Member, IEEE*,
Automation and Control Institute (ACIN), TU Wien
Vienna, Austria
hackl@acin.tuwien.ac.at

Abstract—This paper presents the development of a novel Atomic Force Microscopy mode, enabling dc-bias-free surface potential measurements with high spatial resolution. The influence of the cantilever cone, cantilever beam and lift height in dc-bias-free Kelvin Probe Force Microscopy (AC-KPFM) is reduced due to the proposed heterodyne detection principle, which is sensitive to the electrostatic force gradient. The accuracy of the potential measurement as compared to amplitude modulated KPFM modes is improved, while keeping the advantages of closed-loop and dc-bias-free operation. Measurements on a gold-aluminum test-sample show an increase in spatial resolution of 37% and lift height independent, quantitative surface potential measurements.

Index Terms—kelvin probe force microscopy, surface potential, heterodyne detection, dc-bias-free

I. INTRODUCTION

Kelvin probe force microscopy (KPFM) [1] is an atomic force microscope (AFM) measurement mode for the determination of the local electric surface potential distribution. Electric potentials and charge distributions at the nanoscale are important surface properties as they strongly affect the physical and chemical interaction of the carrier with its environment. KPFM has therefore been used in a variety of scientific fields, such as corrosion studies [2], [3], analysis of semiconductors [4], [5], study of photoconducting devices [6] or biological applications [7], [8]. Especially for the latter, a high spatial resolution is favourable due to the sub-micrometer size of biomolecules.

Many variants of KPFM have evolved [9] most of which use a two-pass technique (interleave mode), where the topography of each scan line is recorded in a first step. The surface potential distribution is then mapped in a subsequent step, where the sample topography is retraced at a constant tip-sample distance (i.e. lift height). The surface potential is measured by modulating the electrostatic interaction of the conducting cantilever to the sample by the application of an ac voltage. The electrostatic force on the tip is nullified by adjusting an additional dc voltage U_{DC} between the cantilever and the sample, directly leading to the surface potential $\phi = U_{DC}$. This so-called amplitude modulated KPFM (AM-KPFM) is sensitive to the long-range electrostatic force on the cantilever. The measurement is therefore not only influenced by the tip

apex, but has also unwanted contribution of sample structures under the cantilever cone and beam, decreasing the spatial resolution. Additionally, the lift height choice determines the contribution of each cantilever part, resulting in lift height dependent measurements and poor potential accuracy. This issue is generally known as averaging effect in amplitude modulated KPFM modes. In contrast to that, frequency modulated (FM) [10] and heterodyne (H) [11] detection techniques have been developed. These modes are sensitive to the gradient of the electrostatic force on the cantilever, which has a faster decline away from the surface than the electrostatic force itself [12]. Therefore, the contribution of the cantilever beam and cone is mitigated, which in turn increases the spatial resolution. Additionally, capacitive signal crosstalk inside the AFM [13], [14], leading to offsets in the feedback loop in AM-KPFM is prevented as the detection frequency is different than the drive frequencies.

Common to all of the above described methods is that they use a dc-bias voltage for the determination of the surface potential distribution. However, in some applications such a dc-bias can deteriorate the measurements or can even have a negative impact on the sample. Semiconductors, often examined by KPFM, show a dependence on the dc voltage as it induces band bending and leads to an invasive measurement [15]. Biological samples often need to be studied in an aqueous solution (in vitro), where the application of a dc-bias would lead to electrochemical reactions or gas formation due to electrolysis [16] making any measurement impossible. There have been efforts to bypass the need for a dc-bias by using open-loop methods [17], [18]. However, such open-loop techniques require an accurate calibration before each measurement. Possible tip pick-up or temperature drifts can make this calibration invalid, leading to hard to interpret or flawed measurements.

Recently the possibility of dc-bias-free closed-loop KPFM has been demonstrated. It uses a second, modulated ac voltage instead of the dc-bias and is known as AC-KPFM [19]. As AC-KPFM is again sensitive to the electrostatic force it can be categorized to amplitude modulated (AM) techniques with all its aforementioned drawbacks.

The contribution of this paper is to extend the AC-KPFM mode with the heterodyne detection principle, in order to increase its resolution and accuracy. As a result measurements on sub-micrometer samples are enabled, where the use of a

The financial support by the Austrian Science Fund FWF (Project Nr. P 31238-N28) and the Austrian Research Promotion Agency FFG (Project Nr. 883916) is gratefully acknowledged.

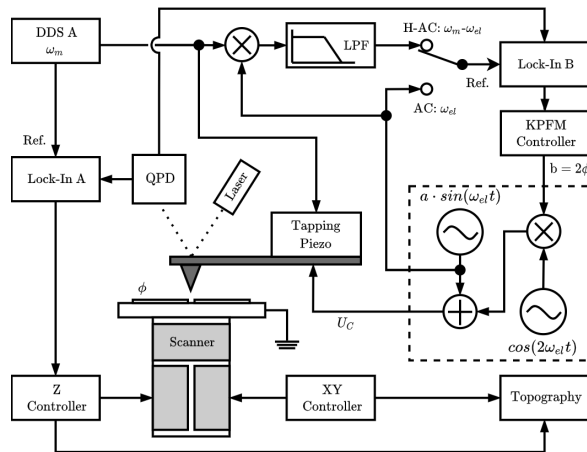


Fig. 1: Implemented H-AC-KPFM setup with the added components on the top left side. DDS A is used for the topography scan and to mechanically excite the cantilever in the interleave scan. A multiplier and a low-pass filter are used to supply Lock-In B with the reference frequency $(\omega_m - \omega_{el})$ for heterodyne detection. A KPFM controller modulates the amplitude b of the following signal generator (dashed box), which provides the AC-KPFM signal U_C . The signal b is recorded and used in a post-processing step to calculate the surface potential map $\phi = b/2$.

dc-bias is detrimental. In the next sections the setup for heterodyne AC-KPFM (H-AC-KPFM) is introduced, its principle is analyzed and experimental details are given. The experimental section includes measurements on a gold-aluminum test sample, where the lift height dependence, measurement accuracy and spatial resolution are analyzed.

II. PRINCIPLE OF HETERODYNE AC-KPFM

In this section, the AC-KPFM [19] technique is presented first, which is then expanded by the heterodyne detection. Fig. 1 shows the setup of AC-KPFM (switch position: down) as well as H-AC-KPFM (switch position: up). These methods operate in a two-pass mode, where in the first pass the topography of a scan line is measured in tapping mode. Subsequently the cantilever follows the recorded topography at a defined lift height above the sample and the surface potential is measured. In AM-KPFM an ac voltage with a dc offset: $U_C = U_{DC} + a \cdot \sin(\omega_{el}t)$ is applied to the cantilever in the second pass, whereas AC-KPFM replaces this dc-bias with an additional sinusoidal signal of twice the frequency:

$$U_C = a \cdot \sin(\omega_{el}t) + b \cdot \cos(2\omega_{el}t). \quad (1)$$

The electrostatic force acting on the tip-sample system is usually expressed as a capacitor model:

$$F_{el} = \frac{1}{2} \frac{\partial C}{\partial z} (\phi - U_C)^2, \quad (2)$$

where $\partial C / \partial z$ is the capacitance gradient between the tip and the sample at the separation z , ϕ is the local surface potential to be measured and U_C the applied voltage on the cantilever. Inserting (1) into (2) leads to various electrostatic force components at several frequencies:

$$F_{el} = \frac{1}{2} \frac{\partial C}{\partial z} \left\{ \begin{array}{l} \phi^2 + \frac{a^2 + b^2}{2} \\ + a[2\phi - b] \sin(\omega_{el}t) \\ - [2\phi b + \frac{a^2}{2}] \cos(2\omega_{el}t) \\ + ab \sin(3\omega_{el}t) \\ + \frac{b^2}{2} \cos(4\omega_{el}t) \end{array} \right\}. \quad (3)$$

AC-KPFM measures the surface potential ϕ by measuring the cantilever deflection amplitude at the frequency ω_{el} (Lock-In B in Fig. 1). A feedback controller is then used to nullify $F_{\omega_{el}}$ by adjusting b , such that $b = 2\phi$. The recorded signal b is then used in a post-processing step to calculate the surface potential $\phi = b/2$. To make use of the high Q-factor of AFM cantilevers and to thus increase the signal-to-noise ratio (SNR), ω_{el} is usually set to the resonance frequency of the cantilever. Next to the advantage that AC-KPFM is dc-bias-free, it also features twice the control sensitivity as compared to conventional AM-KPFM. However, AC-KPFM is equally sensitive to the electrostatic force (see (3)) and features therefore a poor spatial resolution, a lift height dependence and limited potential accuracy arising from the averaging effect.

Heterodyne detection is achieved by exciting the cantilever not only electrically by the application of U_C , but also mechanically during the second pass. By driving the tapping piezo at the frequency ω_m the separation of the cantilever to the sample can be modelled as:

$$z = \bar{z} + A \cdot \sin(\omega_m t), \quad (4)$$

where A is the amplitude of the cantilever deflection at ω_m and \bar{z} is the mean lift height of the cantilever in the interleave scan. The Taylor-Expansion of the tip-sample capacitance gradient is therefore [20]:

$$\frac{\partial C}{\partial z} \approx \left. \frac{\partial C}{\partial z} \right|_{\bar{z}} + A \cdot \left. \frac{\partial^2 C}{\partial z^2} \right|_{\bar{z}} \cdot \sin(\omega_m t). \quad (5)$$

Inserting the altered capacitance gradient (5) into (3) results in frequency mixing of the mechanical and electrical excitation at ω_m and ω_{el} , respectively. The force term at $\omega_m - \omega_{el}$ is used in this implementation and has the following form:

$$F_{\omega_m - \omega_{el}} = \frac{A}{4} \left. \frac{\partial^2 C}{\partial z^2} \right|_{\bar{z}} \cdot a(2\phi - b) \cdot \cos[(\omega_m - \omega_{el})t]. \quad (6)$$

This electrostatic force term leads to a deflection of the cantilever, which again is nullified by controlling b , such that $b = 2\phi$. In contrast to AC-KPFM, the measurement is sensitive to the second derivative of the tip-sample capacitance, which is equivalent to the electrostatic force gradient, instead of the electrostatic force itself. Therefore, heterodyne AC-KPFM mitigates the contribution of the cantilever cone and beam and

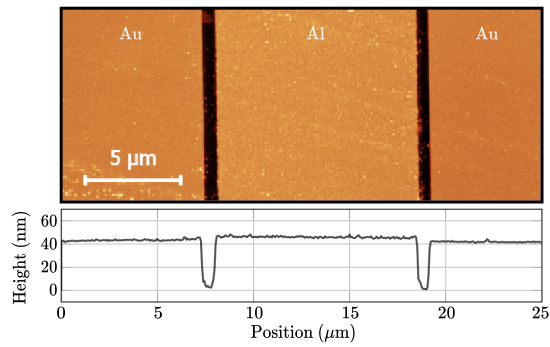


Fig. 2: Tapping mode topography image of the used sample with stripes of varying metal. A representative height profile is shown for clarity.

thus improves the spatial resolution. From Eq. (6) follows that a large mechanical drive amplitude A is favourable in order to get a good SNR. This can be achieved by setting ω_m to the second flexural mode of the cantilever, while keeping $\omega_m - \omega_{el}$ at the fundamental resonance frequency, by an appropriate choice of ω_{el} .

III. SETUP AND EXPERIMENTAL DETAILS

The setup in Fig. 1 is implemented on a commercial AFM (Multimode 8, Bruker, USA) using an external signal generator (33522B, Keysight Technologies, USA) for providing U_C

and an external lock-in-amplifier Lock-In B (SR844, Stanford Research Systems, USA) for the measurement of the deflection amplitude in the interleaved scan. The bandwidth of the lock-in-amplifier is set to 10 kHz and kept constant throughout all measurements. A multiplier followed by a low-pass-filter implemented on a FPGA board (STEMLab 125-14, RedPitaya, Slovenia) are used to generate the reference frequency $\omega_m - \omega_{el}$. A proportional-integral (PI) controller (KPFM controller) implemented on a rapid prototyping system (DS1005, dSpace, Germany) is used to adjust the amplitude b of the AC-KPFM signal, in order to nullify the detected deflection amplitude. The AFM further consists of a Nanoscope V controller and a signal access module (SAM) for the access of specific signals, e.g. the cantilever deflection. The recorded value b is used alongside the topography scan for generating the surface potential map: $\phi = b/2$.

Overall gold coated cantilevers (4XC-GG, Mikromasch, USA) with nominal tip radius of 30 nm, a resonance frequency of $f_0 = 79.8$ kHz and a nominal stiffness of $k = 2.5$ N/m are used in all measurements. For the topography measurement (tapping mode) and the mechanical excitation in the interleave scan, a driving frequency of $\omega_m = 2\pi \cdot 494$ kHz is selected, as the second flexural eigenmode of the cantilever is determined at this frequency. For heterodyne AC-KPFM, the electrical excitation is applied at $\omega_{el} = 2\pi \cdot 414.2$ kHz with an amplitude $a = 2$ V, resulting in a force component at $\omega_m - \omega_{el} = 2\pi \cdot 79.8$ kHz, the resonance frequency of the cantilever. For the use of AC-KPFM an electrical drive frequency of $\omega_{el} = 2\pi \cdot 79.8$ kHz with the same amplitude $a = 2$ V is used.

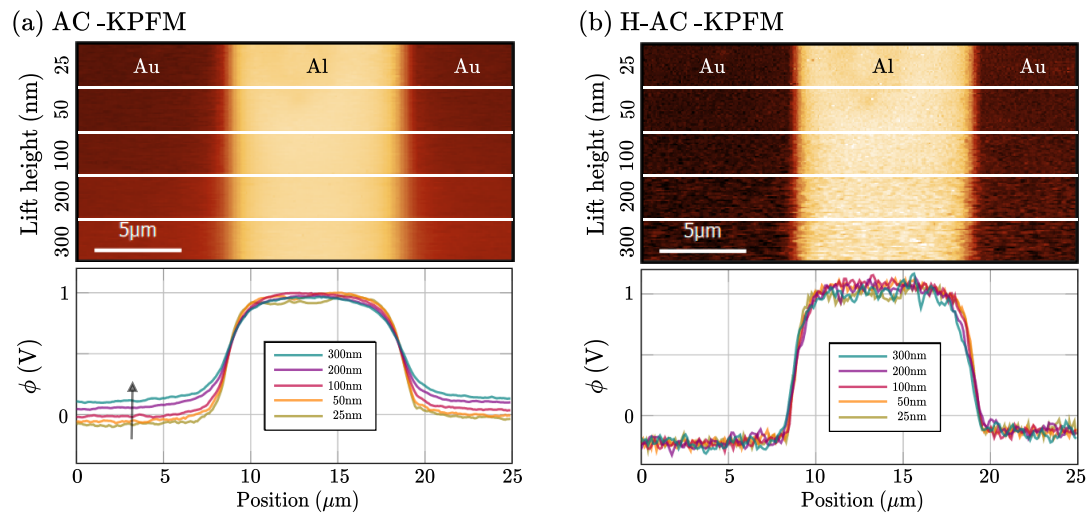


Fig. 3: Sweep of the lift height during the surface potential measurement on the Au-Al-Au sample using (a) AC-KPFM and (b) heterodyne AC-KPFM. The lower graphs show cross sections for each segment in the recorded images, where the arrow denotes the direction of increased lift height. Changing the lift height has a major impact on the measurement result of force-sensitive AC-KPFM, whereas with heterodyne AC-KPFM this artefact is not present.

The method is verified on a test-sample (KPFM & EFM Sample, BudgetSensors, Bulgaria), which features stripes of alternating materials (aluminum and gold) on an oxide covered silicon substrate separated by a 500 nm wide trench. The height of the stripes is almost identical (see Fig. 2), therefore minimizing possible topographical crosstalk in the measurement. A surface potential contrast arises from the different work functions of the materials, creating a contact potential difference. Additionally an external bias can be applied to either material to set a known potential difference.

IV. EXPERIMENTAL COMPARISON OF AC-KPFM AND H-AC-KPFM

A. Lift height dependence

In Fig. 3 the measured surface potential, when sweeping the lift height from 25 nm up to 300 nm for conventional AC-KPFM (a) and H-AC-KPFM (b) is shown. The cross sections show a clear dependence on lift height when operating with AC-KPFM. As discussed in the introduction, the long-range electrostatic force not only acts on the tip apex but also on the cantilever cone and beam. In the experiment the cantilever beam extends over the Al-pad. Meaning, that when increasing the distance to the surface and therefore also the contribution of the beam, the measured potential on the Au-pad approaches the value of the Al-pad. A careful choice of the lift height and the cantilever direction is therefore essential, when operating with amplitude modulated KPFM modes to deal with this cantilever and lift height induced artefact.

Heterodyne AC-KPFM on the other hand is not influenced by the choice of the lift height due to its proportionality to the more localized electrostatic force gradient. Even at large distances (i.e. 300 nm) above the sample it provides the same quantitative result as for small lift heights and is thus less prone to variations of measurement parameters. Along with this advantage comes a drawback of the heterodyne detection. As the electrostatic force gradient features a rapid decline away from the surface, large lift heights lead to small forces and therefore a reduced SNR. However, the SNR can be noticeably enhanced by either increasing the mechanical or the electrical drive amplitude A and a , respectively (as described by (6)) and by selecting the lift height small enough.

B. Voltage accuracy and spatial resolution

Fig. 4 shows the measured surface potential on the same position as in the previous section at a lift height of 25 nm when sweeping the external bias voltage on the Al-pad, while keeping the Au-pad at ground potential. With AC-KPFM the measured surface potential between the +1 V and -1 V plateau on the Al-pad is clearly less than 2 V. This is again attributed to the averaging effect present in amplitude modulated KPFM modes. Additionally, capacitive signal crosstalk can induce an offset in the feedback loop, leading to erroneous results. With H-AC-KPFM on the other side the detection frequency ($\omega_m - \omega_{el}$) is different from the drive frequencies (ω_m, ω_{el}). Eventual crosstalk is therefore not influencing the measurement, as it is filtered by the narrow bandwidth of the lock-in-amplifier. It is shown that the measured potential with H-

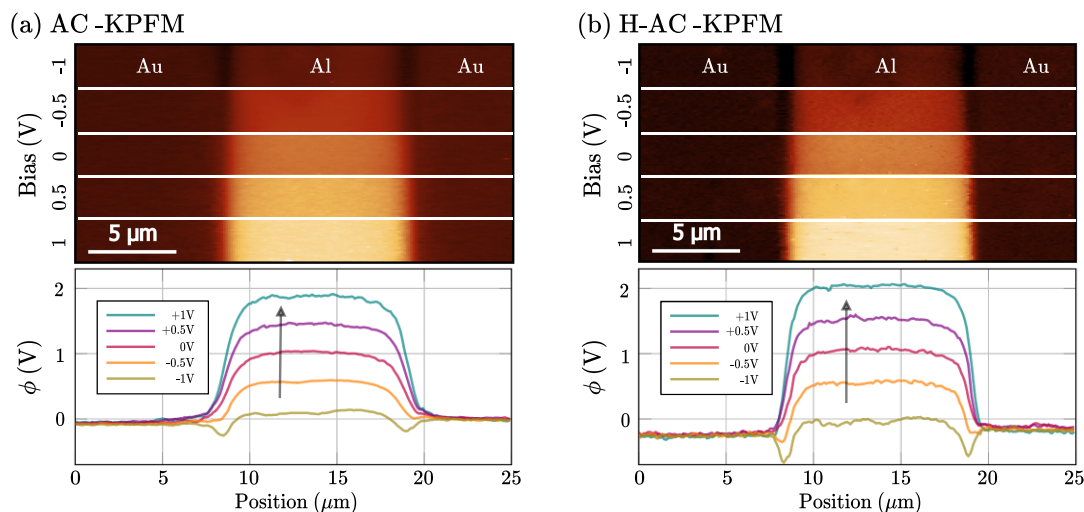


Fig. 4: Sweep of the externally applied bias voltage on the Al pad, while keeping the Au potential on ground for (a) AC-KPFM and (b) heterodyne AC-KPFM (lift height = 25 nm). The cross section of each segment is given in the lower graphs, where the arrows denote the direction of increased bias. Due to averaging in amplitude modulated AC-KPFM the applied voltages are not accurately measured as the difference of the -1 V and +1 V lines on the Al pad is less than 2 V. For heterodyne detection on the other hand the quantitative correct potentials are measured.

AC-KPFM follows accurately the applied 0.5 V voltage steps. Additionally to the quantitatively correct surface potential measurement, heterodyne AC-KPFM indicates an increased spatial resolution visible through the more pronounced dip in the -1 V potential curve. It arises from the different contact potential of the underlying oxide covered silicon substrate that is exposed at the transition. The increased resolution can also be seen by the steeper transition of the other curves. The rise width (10%-90%) of the measured surface potential (+1 V) is determined to be 1.99 μm for AC-KPFM and 1.25 μm for H-AC-KPFM, which is an improvement of 37% at a lift height of 25 nm.

In summary, the proposed dc-bias-free closed-loop KPFM method is successfully presented and features a lift height independent and quantitatively correct surface potential measurement with high spatial resolution.

V. CONCLUSION

The heterodyne AC-KPFM technique introduced in this paper increases the spatial resolution and measurement accuracy as compared to conventional KPFM modes, all while operating dc-bias-free, in a closed-loop and without the need for a calibration. This novel method is sensitive to electrostatic force gradients rather than forces, such as in amplitude modulated KPFM modes (i.e. AM-KPFM). Therefore, diminishing the averaging effect of the cantilever cone and cantilever beam in surface potential measurements. This makes the measurement solely depending on the localised force at the very tip, resulting in a lift height independent measurement with high potential accuracy. Furthermore, with heterodyne detection the detection frequency is a mixing component of the mechanical and electrical drive frequencies, which reduces cross-talk induced feedback-artefacts in the surface potential measurement.

The results demonstrate that heterodyne AC-KPFM has the capability of quantitative surface potential measurements with high spatial resolution on samples and environments, where the use of a dc-bias is not possible. This mode therefore opens the way for measurements on semiconductors or biological samples, where the use of a dc-bias is detrimental and sub-micrometer structures need to be investigated.

REFERENCES

- [1] M. Nonnenmacher, M. P. O'Boyle, and H. K. Wickramasinghe, "Kelvin probe force microscopy," *Applied Physics Letters*, vol. 58, no. 25, pp. 2921–2923, 1991.
- [2] M. Rohwerder and F. Turcu, "High-resolution kelvin probe microscopy in corrosion science: Scanning kelvin probe force microscopy (skpfm) versus classical scanning kelvin probe (skp)," *Electrochimica Acta*, vol. 53, no. 2, pp. 290–299, 2007.
- [3] C. Örnek, C. Leygraf, and J. Pan, "Real-time corrosion monitoring of aluminum alloy using scanning kelvin probe force microscopy," *Journal of the Electrochemical Society*, vol. 167, no. 8, p. 081502, 2020.
- [4] Y. Rosenwaks, R. Shikler, T. Glatzel, and S. Sadewasser, "Kelvin probe force microscopy of semiconductor surface defects," *Phys. Rev. B*, vol. 70, p. 085320, 2004.
- [5] S. Saraf and Y. Rosenwaks, "Local measurement of semiconductor band bending and surface charge using kelvin probe force microscopy," *Surface Science*, vol. 574, no. 2, pp. L35–L39, 2005.
- [6] E. Sengupta, A. L. Domanski, S. A. L. Weber, M. B. Untch, H.-J. Butt, T. Sauer mann, H. J. Egelhaaf, and R. Berger, "Photoinduced degradation studies of organic solar cell materials using kelvin probe force and conductive scanning force microscopy," *The Journal of Physical Chemistry C*, vol. 115, no. 40, pp. 19994–20001, 2011.
- [7] A. K. Sinensky and A. M. Belcher, "Label-free and high-resolution protein/dna nanoarray analysis using kelvin probe force microscopy," *Nature nanotechnology*, vol. 2, no. 10, pp. 653–659, 2007.
- [8] P. Mesquida, D. Kohl, O. G. Andriotis, P. J. Thurner, M. Duer, S. Bando, and G. Schitter, "Evaluation of surface charge shift of collagen fibrils exposed to glutaraldehyde," *Scientific reports*, vol. 8, no. 1, p. 10126, 2018.
- [9] L. Collins, J. I. Kilpatrick, S. V. Kalinin, and B. J. Rodriguez, "Towards nanoscale electrical measurements in liquid by advanced KPFM techniques: a review," *Reports on Progress in Physics*, vol. 81, no. 8, p. 086101, 2018.
- [10] T. Glatzel, S. Sadewasser, and M. Lux-Steiner, "Amplitude or frequency modulation-detection in kelvin probe force microscopy," *Applied Surface Science*, vol. 210, no. 1–2, pp. 84–89, 2003.
- [11] Z. M. Ma, L. Kou, Y. Naitoh, Y. J. Li, and Y. Sugawara, "The stray capacitance effect in kelvin probe force microscopy using fm, am and heterodyne am modes," *Nanotechnology*, vol. 24, no. 22, p. 225701, 2013.
- [12] J. L. Garrett, M. S. Leite, and J. N. Munday, "Multiscale functional imaging of interfaces through atomic force microscopy using harmonic mixing," *ACS Applied Materials & Interfaces*, vol. 10, no. 34, pp. 28850–28859, 2018.
- [13] S. Barbet, M. Popoff, H. Diesinger, D. Deresmes, D. Théron, and T. Mélin, "Cross-talk artefacts in kelvin probe force microscopy imaging: A comprehensive study," *Journal of Applied Physics*, vol. 115, no. 14, p. 144313, 2014.
- [14] P. Mesquida, D. Kohl, and G. Schitter, "Signal reversal in kelvin-probe force microscopy," *The Review of scientific instruments*, vol. 90, no. 11, p. 113703, 2019.
- [15] J. Xu and D. Chen, "Interpreting kelvin probe force microscopy on semiconductors by fourier analysis," *Journal of Applied Physics*, vol. 129, no. 3, p. 034301, 2021.
- [16] L. Collins, S. Jesse, J. I. Kilpatrick, A. Tselev, M. B. Okatan, S. V. Kalinin, and B. J. Rodriguez, "Kelvin probe force microscopy in liquid using electrochemical force microscopy," *Beilstein journal of nanotechnology*, vol. 6, pp. 201–214, 2015.
- [17] N. Kobayashi, H. Asakawa, and T. Fukuma, "Dual frequency open-loop electric potential microscopy for local potential measurements in electrolyte solution with high ionic strength," *The Review of scientific instruments*, vol. 83, no. 3, p. 033709, 2012.
- [18] K. Honbo, S. Ogata, T. Kitagawa, T. Okamoto, N. Kobayashi, I. Sugimoto, S. Shima, A. Fukunaga, C. Takato, and T. Fukuma, "Visualizing nanoscale distribution of corrosion cells by open-loop electric potential microscopy," *ACS nano*, vol. 10, no. 2, pp. 2575–2583, 2016.
- [19] D. Kohl, P. Mesquida, and G. Schitter, "Quantitative ac - kelvin probe force microscopy," *Microelectronic Engineering*, vol. 176, pp. 28–32, 2017.
- [20] J. L. Garrett, D. Somers, and J. N. Munday, "The effect of patch potentials in casimir force measurements determined by heterodyne kelvin probe force microscopy," *Journal of physics. Condensed matter: an Institute of Physics journal*, vol. 27, no. 21, p. 214012, 2015.